

# Non-Coherent UWB Communications

Mike Wolf, Nuan Song, and Martin Haardt

**Abstract** – Non-coherent receivers have become promising candidates for low complexity and low power ultra wide band (UWB) systems. We discuss the performance of energy detection and differential detection in additive white Gaussian noise, Rayleigh fading, and multipath environments. It is shown that non-coherent receivers can easily collect the multipath energy by means of equal gain combining. The loss (compared to quite hypothetical coherent channel matched filter detection) which is introduced by this suboptimal combining technique is tolerable, if the receiver utilizes a filter matched to the transmitted waveform. A system concept for low data rate communications based on frequency hopping and complete digital baseband processing is also presented.

**Index Terms** – low data rate, UWB, non-coherent, small scale fading, matched filter, analog-to-digital converter, frequency hopping, differential OFDM

## 1 Introduction

In Feb. 2002, the US federal communications commission (FCC) permitted the operation of UWB transmitters in the frequency band from 3.1 to 10.6 GHz at an effective isotropic radiated power spectral density of -41.3 dBm/MHz [1]. In the past, many original UWB system designs targeted to use the whole available bandwidth of 7.5 GHz at once via the emission of very short sub-nanosecond pulses.

A large bandwidth – in case of UWB at least 500 MHz – has many benefits for communications. It can provide a very robust performance even under harsh multipath and interference conditions, the capability of precision ranging and a reduced power consumption. Since the power spectral density is very low, it is possible to overlay UWB networks with already existing non-UWB emissions.

Nevertheless, some serious problems will also occur if the signal bandwidth is increased more and more. These problems are related to the transceiver components themselves (availability of broadband antennas, amplifiers etc.), and to the technical effort which is required for synchronization, channel estimation, and interference rejection. Since UWB networks operate in frequency bands already assigned to other RF-systems, the probability that narrowband interference occurs at all increases with the bandwidth, too. Furthermore, by increasing the bandwidth, more and more multipath arrivals with different path gains and delays are resolvable at the receiver, which makes it difficult to collect the multipath energy coherently, although the receive power at the antenna input does not suffer from the fading effect.

Early UWB approaches have almost exclusively relied upon carrier-less time hopping impulse radio. However, by taking into account the bandwidth related challenges and also important changes in the UWB-regulation<sup>1</sup>, it is not astonishing that a lot of alternative concepts like orthogonal frequency division multiplex (OFDM) [5], frequency hopping (FH) [6], chirp or direct-sequence spread spectrum modulation [7] have been demonstrated recently.

This paper focuses on non-coherent UWB transmission, which is an attractive candidate especially if simple and robust implementations with small power consumption are required [8]. It should be noted that the current IEEE 802.15.4a UWB Physical layer for low data rate personal area and sensor networks [9] has been developed such that it enables non-

coherent detection, too. A non-coherent detector can collect the multipath energy very easily by means of equal gain combining, i. e., by means of a simple integrator and without any channel estimation. Compared to coherent solutions, the effort with respect to the receiver synchronization is considerably reduced.

Non-coherent detection can either rely on energy/envelope detection or on differential detection. With respect to energy detection, we consider an orthogonal binary pulse-position modulation (2-PPM) system. 2-PPM is the "essential" modulation for the IEEE 802.15.4a UWB PHY<sup>2</sup>. Differential detection requires either differential phase-modulation or transmit-reference signaling (TR). In the second case, the phase of the current modulated symbol is not compared to the previous one but to an unmodulated reference pulse. We choose differential binary phase-shift keying (DPSK) exemplarily, and discuss TR in Section 3.2, too.

## 2 Modulation and Detection

### 2.1 2-PPM Energy Detection

If  $E_b$  denotes the mean energy per bit, a 2-PPM signal (single carrier with fixed carrier frequency) given in the complex baseband can be written as

$$s(t) = \sqrt{E_b} \sum_{n=-\infty}^{\infty} (1 - b_n)\psi_0(t - nT_b) + b_n\psi_1(t - nT_b), \quad (1)$$

where  $\psi_1(t) = \psi_0(t - T_b/2)$  needs to be orthogonal to  $\psi_0(t)$ .  $T_b$  is the bit interval, which is split into two subintervals each of length  $T_b/2$ . Depending on the binary information  $b_n$ ,  $b_n \in \{0, 1\}$ , to be transmitted, the waveform  $\sqrt{E_b}\psi_0(t)$  is generated either at the time  $T_b$  or  $T_b/2$  seconds later. For single carrier transmission with a fixed carrier frequency, the unit energy basis function  $\psi_0(t)$  needs to exhibit a bandwidth of at least 500 MHz, i. e., it is a spread spectrum waveform. For example, according to the IEEE 802.15.4a UWB PHY,  $\psi_0(t)$  consists of a single pulse with a duration of 2 ns (or less) or a burst of up to 128 such pulses with a scrambled polarity. The burst duration is much smaller than  $T_b$ .

The block diagram of an energy detection receiver is shown in Fig. 1 a). It is important to note that the system is still modeled in the complex baseband. A "true" detector would either require an additional quadrature down-conversion

<sup>1</sup> In Europe, beginning with 2011, -41.3 dBm/MHz is permitted only between 6 and 8.5 GHz, if no detect and avoid (DA) techniques are implemented [2]. With DA, -41.3 dBm/MHz is also permitted between 4.2 and 4.8 GHz [3]. Both in the US [4] as well as in Europe the regulation is now technology independent.

<sup>2</sup> Binary Phase Shift Keying is also used, but only to convey a redundant bit created by a systematic convolutional code. This bit may be used for error detection if coherent detection is used.

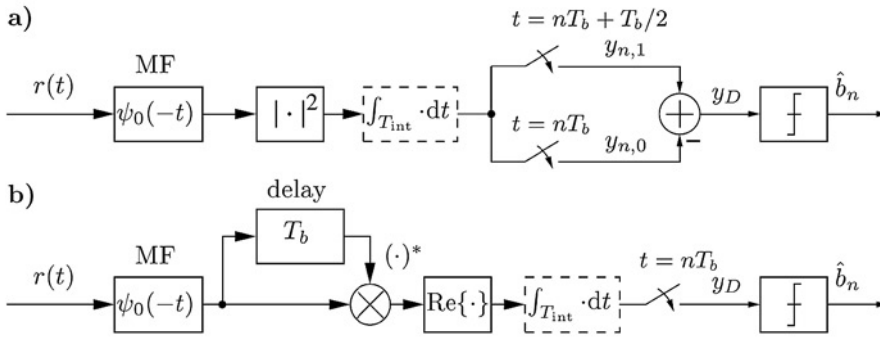


Fig. 1: Non-coherent receiver models shown in the complex baseband: a) 2-PPM energy detection (soft-decision), b) DPSK differential detection. The integrator (dashed box) can be omitted, if the receiver can not resolve multipath arrivals.

stage (with the inphase and the quadrature components being the real and the imaginary part of the received signal) or an additional bandpass filter at its input. It is assumed that the receiver utilizes a filter which is matched to the transmitted signal  $\psi_0(t)$ . Without multipath, this ensures that the energy  $E_b$  of the received signal  $r(t)$  is focused either at the sampling time  $nT_b$  or  $T_b/2$  seconds later. With multipath, it ensures that the energy dispersion at the filter output is only caused by the multipath propagation itself, see Section 3.3. For example, according to the IEEE 802.15.4a UWB PHY a receiver needs to perform a matched de-chirp operation, if the optional "chirp on UWB" pulse is used.

The main difference compared to coherent detection is the squaring device, which removes any phase/polarity. This enables the usage of an integrator for equal gain combining of the multipath arrivals, where the integration time depends on the delay spread of the channel.

## 2.2 DPSK Differential Detection

A (single carrier) DPSK signal given in the complex baseband can be written as

$$s(t) = \sqrt{E_b} \sum_{n=-\infty}^{\infty} (2\tilde{b}_n - 1)\psi_0(t - nT_b), \quad (2)$$

where  $\tilde{b}_n = b_n \oplus \tilde{b}_{n-1}$ ,  $\tilde{b}_n \in \{0, 1\}$ , denotes differentially encoded bits.

The corresponding receiver block diagram is shown in Fig. 1 b). In this case, the phase/polarity is removed by multiplying the received (and filtered) signal with its complex conjugated, delayed version. For differential modulation, the delay needs to be as large as the symbol interval (or multiples of the symbol interval, if non-adjacent bits are used to build  $\tilde{b}_n$ ). This renders analog realizations of the receiver rather difficult or even impossible, since delays with a huge delay-bandwidth product are required. Furthermore, analog realizations would require two of those delays, if quadrature down-conversion is used. If the delay takes place on the received bandpass signal (as in fiber optical DPSK receivers), then only one delay line is required, but the delay accuracy needs to be much more precise than  $1/f_c$ , where  $f_c$  is the carrier frequency.

There are several solutions to solve this problem. One is TR signaling [10], which has been intensively discussed in the UWB community. In this case, the modulated symbol is not compared with the previous one but with a reference pulse additionally transmitted within  $T_b$ . This approach reduces the delay bandwidth product at the cost of a 3 dB loss caused by the unmodulated reference and a further loss caused by multipath induced intra-symbol interference [8].

Another possibility would be to sample the signal prior to the delay or prior to the matched filter, which requires high speed analog-to-digital converters instead of "high speed" delays. It should be noted that differential UWB does not

require spread spectrum signals. Differential phase modulation is also well suited for OFDM, which will be discussed in Section 3.2. In this case, the main parts of the receiver are also completely digital.

## 3 Performance Analysis

### 3.1 Performance in AWGN

The  $E_b/N_0$ -performance in ideal AWGN acts as a benchmark performance ( $N_0$  is the technical noise power spectral density). A non-coherent UWB receiver operating in multipath may nearly achieve this reference performance, if a strong line-of-sight path exists. In this case, the integrator can be omitted.

It is beyond the scope of this contribution to derive the bit error rate (BER)  $p_b$  of non-coherently detected 2-PPM and DPSK, since the derivations can be found elsewhere [11]. The results are shown in Table 1 and Fig. 2. However, it is remarkable to note that the decision variable  $y_D$  shown in Fig. 1 a) for 2-PPM energy detection exhibits exactly the same statistic as the one shown in Fig. 1 b) for differential DPSK detection, except that the parameter  $N_0$  needs to be replaced by  $N_0/2$  in the latter case [10], i. e., DPSK outperforms 2-PPM by 3 dB.

Fig. 2 shows that at  $p_b = 10^{-3}$ , non-coherent detection introduces a  $E_b/N_0$  performance loss of approximately 1.2 dB compared to coherent detection.

### 3.2 Performance in Rayleigh Fading

The results in AWGN can be used to estimate the performance of time differential OFDM-transmission, where each OFDM-symbol is differentially encoded with respect to the previous one.

For OFDM, the detection of each sub-carrier is only affected by flat fading and AWGN, if the duration of the cyclic prefix is as long as the channel delay spread and if other impairments such as synchronization errors or non-linearities do not occur. Assuming Rayleigh fading (i. e., there are no dominating transmission paths) with respect to the amplitude characteristic in the frequency domain and a total bandwidth which is large compared to the coherence bandwidth of the channel, the BER averaged over all subcarriers can be expressed as in Table 1, [12].

Fig. 2 shows that the performance compared to coherent multicarrier detection (see Table 1, [12]) suffers by less than 3 dB. In [13] it is shown that differentially detected D-QPSK may even outperform coherently detected QPSK, if a carrier offset is considered.

Whereas differential OFDM is an attractive candidate for very high data rates, FH combined with energy detection can

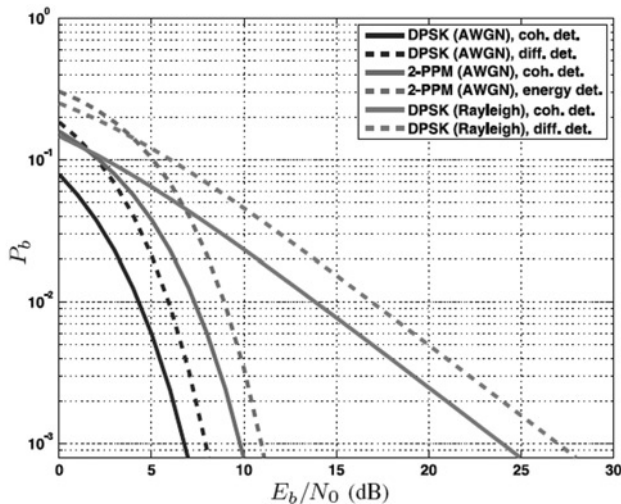


Fig. 2: BER in AWGN and Rayleigh-fading (no coding).

Table 1: BER in AWGN and Rayleigh-Fading Channels

	2-PPM (AWGN)	DPSK (AWGN)	DPSK (Rayleigh)
Non-Coherent	$\frac{1}{2} \exp\left(-\frac{E_b}{2N_0}\right)$	$\frac{1}{2} \exp\left(-\frac{E_b}{N_0}\right)$	$\frac{1}{2\left(\frac{E_b}{N_0} + 1\right)}$
Coherent	$Q\left(\sqrt{\frac{E_b}{N_0}}\right)$	$Q\left(\sqrt{\frac{2E_b}{N_0}}\right)$	$\frac{1}{2}\left(1 - \sqrt{\frac{E_b/N_0}{1 + E_b/N_0}}\right)$

be seen as a – very similar – counterpart for low data rates<sup>3</sup>. For 2-PPM, the transmitted signal can be represented by

$$s(t) \cdot \exp(j2\pi c_k \Delta f t), \quad k = \lfloor t/T_b \rfloor, \quad c_k \in \{0, 1, \dots, N_{\text{hop}} - 1\}, \quad (3)$$

where  $s(t)$  is given in Eqn. (1). The term  $c_k$  denotes the FH code,  $\Delta f$  is the frequency spacing. The main difference compared to OFDM is that  $N_{\text{hop}}$  different sub-channels are not used in parallel but subsequently, which reduces the data rate by the same factor  $N_{\text{hop}}$ . If  $N_{\text{hop}}$  non overlapping channels are used, the bandwidth with respect to  $\psi_0(t)$  is reduced by  $N_{\text{hop}}$ , too, which enables complete digital solutions for the 2-PPM baseband receiver as in [14]. The technical effort for the down-conversion can be kept small, since the oscillator at the receive site can be free running.

### 3.3 Performance in Multipath

In Section 3.1, non-coherent detection in AWGN is discussed. It is assumed that a filter matched to  $\psi_0(t)$  is utilized, which ensures that the whole bit energy is focused at the sampling time. In this case, the detector performance is independent of the concrete shape of  $\psi_0(t)$ .

We now incorporate multipath propagation, where we assume that a filter matched to  $\psi_0(t)$  is still utilized at the receiver. Multipath propagation will lead to an energy dispersion at the filter output, if several propagation paths are resolvable, i.e., if the product of the (baseband) signal bandwidth  $B$  and the excess delay of the channel is larger than 1. For example, with  $B = 500$  MHz and an assumed excess delay of 50 ns, about 25 individual paths are resolvable in the time domain. To collect the energy  $E_b$  of all these multipath arrivals without any channel knowledge, equal gain combin-

ing can be performed over the whole window of  $T_{\text{int}}$  ns by means of the integrator shown in Fig. 1.

In contrast to a matched filter that combines all signal components coherently and with an appropriate weighting, the integrator clearly allows only non-coherent combining. Compared to a – rather hypothetical – coherent receiver which employs a channel matched filter this suboptimal combining leads to a performance loss, which increases with the product  $B \cdot T_{\text{int}}$  [15, 16]. If we assume that the whole bit energy  $E_b$  is contained within the integration interval  $T_{\text{int}}$ , and if we further assume that  $B \cdot T_{\text{int}}$  is an integer  $N \geq 1$ , the BER for 2-PPM can now be estimated as [17]

$$p_b = \frac{1}{2^N} \exp\left(-\frac{E_b}{2N_0}\right) \sum_{i=0}^{N-1} \frac{1}{2^i} L_i^{N-1}\left(-\frac{E_b}{2N_0}\right) \approx Q\left(\frac{E_b/N_0}{\sqrt{2E_b/N_0 + 2N}}\right), \quad (4)$$

where  $L_i^{N-1}$  is a generalized Laguerre polynomial. The right expression corresponds to a Gaussian approximation which can be used for large  $N$  ( $N \geq 15$ ). For DPSK,  $N_0$  should be replaced by  $N_0/2$ . Eqn. (4) is only valid if no inter symbol interference (ISI) occurs, which is the case if the channel excess delay is small compared to  $T_b$ .

Fig. 3 shows the penalty with respect to the required  $E_b/N_0$ , if we switch from the hypothetical coherent channel matched filter detection to non-coherent detection with equal gain combining. A value of 1.2 dB at  $N = 1$  just corresponds to the  $E_b/N_0$ -penalty in AWGN at  $p_b = 10^{-3}$ , cf. Fig. 2. The results must be interpreted very carefully, since it is assumed that the whole bit energy is concentrated within the interval  $T_{\text{int}}$ . In reality, this is not the case and an appropriate  $T_{\text{int}}$  must be found. If  $T_{\text{int}}$  is increased, more and more noise is integrated which leads to the loss shown in Fig. 3, but more signal energy may be collected as well. The influence of  $T_{\text{int}}$  on  $p_b$  is shown in Fig. 4 for a measured non-LOS indoor channel (office) [18].

An appropriate bandwidth  $B$  must be chosen as well. A good small scale fading resistance just requires a certain minimum bandwidth  $B$ , so that the propagation paths are resolvable in the time domain. Otherwise, the multipath arrivals interfere coherently which may lead to deep fades. Therefore, a good single carrier system design has to choose a value for  $B$  which guarantees a good trade-off between the fading resistance and the combining loss. Our analysis shows that even indoors, where we have a small excess delay and hence a large coherence bandwidth, a bandwidth  $B > 200$  MHz is not desirable from the required  $E_b/N_0$  point of view.

If multiple carriers are used in parallel (OFDM) or subsequently (FH),  $B$  can clearly be much smaller, since the fading resistance is not only obtained by path diversity but also by frequency diversity. This approach that enables complete digital baseband processing as in [14] will be outlined in the next section.

## 4. System Concept for Low Data Rates

The main purpose of the UKoLoS project "Low-Complexity UWB Communication" is the development of non-coherent physical layer concepts for low data rates systems. The network/multiuser aspect has not been discussed until now, but it can be easily verified that a non-coherent receiver will not achieve the interference resistance of a coherent one. With increasing  $T_{\text{int}}$ , more and more multiuser and narrow-band interference will be received, too.

Within UKoLoS, we favour a FH approach with complete digital baseband processing. FH is standard conform, if a bandwidth of at least 500 MHz is covered within 1 ms, which can be easily achieved in practice. FH has several major

<sup>3</sup> Since the channel changes with every new carrier frequency, FH-DPSK requires a delay equal to the period of the FH code, which may be larger than the coherence time of the channel. This depends on the application (mobility) and on the period of the FH code.

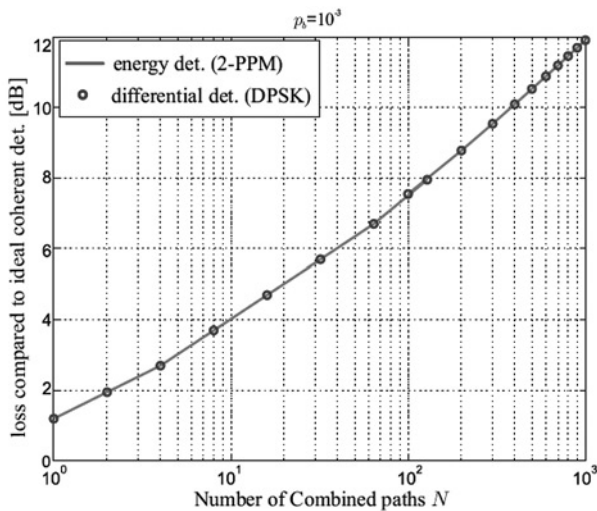


Fig. 3: Non-coherent combining loss depending on the time bandwidth product  $N$ . Coherent channel matched filter detection (2-PPM/DPSK) acts as the reference.

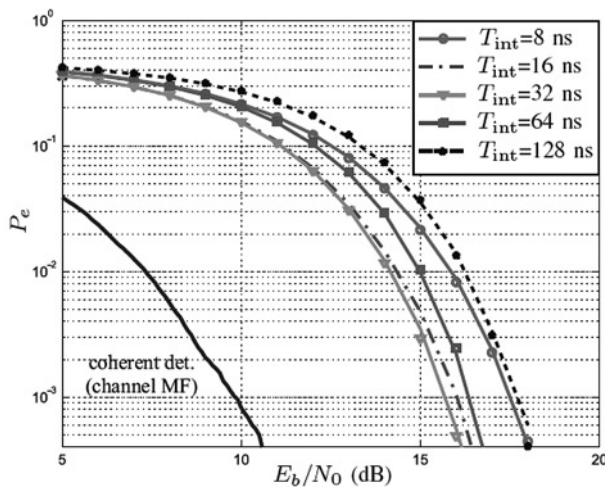


Fig. 4: BER performance of non-coherently detected 2-PPM for different  $T_{\text{int}}$  and a measured indoor channel ( $B = 500$  MHz).

advantages. It provides a very good spectral control, it enables detect and avoid, it provides a very good interference resistance, it does not suffer from the near-far effect, and it reduces the baseband bandwidth  $B$ . With respect to  $B$ , we favour values between 20 and 100 MHz, which enable the usage of low cost analog-to-digital (AD)-converters. Since non-coherent detection is used, which is tolerant to frequency offsets, even the technical effort for the down-conversion is low.

Complete digital baseband processing has several advantages, too. It ensures that a filter matched to the transmitted waveform  $\psi_0(t)$  can be implemented in practice, which restricts the combining loss to the multipath arrivals only. Since the multipath resolution capability is reduced by reducing  $B$ , even a non-coherent Rake with weighted combining can be implemented.

Furthermore, a digital receiver can easily distinguish different spreading signals  $\psi_0(t)$ , which are assigned to different users or networks. With respect to the modulation scheme, orthogonal Walsh-modulation with hard detection is preferred.

## 5 Conclusions

The  $E_b/N_0$  performance of non-coherently detected 2-PPM and DPSK is very similar. It differs by 3 dB in favour of DPSK. In AWGN, non-coherent detection exhibits a loss of about 1.2 dB compared to coherent detection. In Rayleigh-fading, which is an appropriate model for differential OFDM and "pure" FH-systems (baseband bandwidth on the order of the channel coherence bandwidth or less), the difference compared to coherent detection is increased to about 3 dB. Non-coherent multipath combining introduces a loss compared to ideal coherent detection (channel matched filter), which increases with the delay spread of the channel as well as with the bandwidth. Since the fading resistance depends on the bandwidth, too, a good system design has to choose the baseband bandwidth very carefully. Frequency hopping systems are promising candidates for low data rate communications. They provide a mixture between path and frequency diversity, enable digital low cost solutions for the baseband processing, and are immune to interference.

## References

- [1] FCC 02–48, "Revision of Part 15 of the Commission's Rules Regarding Ultra-Wideband Transmission Systems," ET Docket 98–153, Apr. 2002.
- [2] ECC, "ECC Decision of 24 March 2006 amended 6 July 2007 at Constanta on the harmonised conditions for devices using Ultra-Wideband (UWB) technology in bands below 10.6 GHz," amended ECC/DEC/(06)04, July 2007.
- [3] ECC, "Final report on UWB in response to a request from the European Commission," Doc. ECC (08)023 Annex12, Mar. 2008.
- [4] FCC 05–58, "Petition for Waiver of the Part 15 UWB Regulations Filed by the Multi-band OFDM Alliance Special Interest Group," ET Docket 04–352, Mar. 2005.
- [5] A. Batra et al., "Multi-band OFDM Physical Layer Proposal for IEEE 802.15 Task Group 3a," Sept. 2003, Document No. IEEE P802.15–03/268r1.
- [6] Public Safety Communication Europe, "D.4.1.1. Public Report EUROPCOM (Emergency Ultrawideband RadiO for Positioning and Communications), Summary of the System Architecture, Issue 1," project no. 004154, June 2006.
- [7] I. Oppermann, L. Stoica, A. Rabbachin, Z. Shelby, and J. Haapola, "UWB Wireless Sensor Networks: UWEN—A Practical Example," *IEEE Radio Communications*, pp. S27–S32, Dec. 2004.
- [8] K. Witrisal, G. Leus, G. J. M. Janssen, M. Pausini, F. Trösch, T. Zasowski, and J. Romme, "Noncoherent Ultra-Wideband Systems: An Overview of Recent Research Activities," *IEEE Signal Processing Magazine*, pp. 48–66, July 2009.
- [9] IEEE Std. 802.14.4a 2007, "Wireless Medium Access Control (MAC) and Physical Layer (PHY) Specifications for Low-Rate Wireless Personal Area Networks (WPANs), Amendment 1: Add Alternate PHYs," Aug. 2007.
- [10] T. Q. S. Quek and M. Z. Win, "Analysis of UWB transmitted-reference communication systems in dense multipath channels," *IEEE Journal on Selected Areas in Communications*, no. 9, pp. 1863–1874, 2005.
- [11] J. G. Proakis and M. Salehi, *Communication Systems Engineering*, Prentice Hall, 2nd edition, 2002.
- [12] S. Haykin, *Communication Systems*, John Wiley & Sons, 4th edition, 2001.
- [13] S. Islam and N. Al-Dhahir, "A High-Performance Double Differential OFDM UWB Receiver," in *Asilomar Conference on Signals, Systems and Computers, ACSSC'06*, Oct. 2006, pp. 1733–1737.
- [14] N. Song, M. Wolf, and M. Haardt, "A Digital Code Matched Filter-based Non-Coherent Receiver for Low Data Rate TH-PPM-UWB Systems in the Presence of MUI," in *Proc. of IEEE 2009 International Conference on UltraWideband, ICUWB'09*, Vancouver, Canada, Sept. 2009.
- [15] M. Wolf and N. Song, "Chapter 5: Non-Coherent Detection," in *Short-Range Wireless Communications: Emerging Technologies and Applications*, R. Kraemer and M. D. Katz, Eds. Wiley, 2009.
- [16] N. Song, M. Wolf, and M. Haardt, "Performance of PPM-Based Non-Coherent Impulse Radio UWB Systems using Sparse Codes in the Presence of Multi-User Interference," in *Proc. of IEEE Wireless Communications and Networking Conference, WCNC'09*, Budapest, Hungary, April 2009.
- [17] M. J. Hao and S. B. Wicker, "Performance evaluation of FSK and CPFSK optical communication systems: a stable and accurate

method," *Journal of lightwave technology*, no. 13, pp. 1613–1623, 1995.

- [18] N. Song, M. Wolf, and M. Haardt, "Low-complexity and Energy Efficient Non-coherent Receivers for UWB Communications," in *Proc. of 18-th Annual IEEE International Symposium on Personal Indoor and Mobile Radio Communications, PIMRC'07*, 2007

Mike Wolf, Nuan Song, and Martin Haardt  
Communication Research Laboratory  
Ilmenau University of Technology  
P.O. Box 100565, D-98693 Ilmenau, Germany  
Web page: [www.tu-ilmenau.de/crl](http://www.tu-ilmenau.de/crl)  
Email: {mike.wolf, nuan.song, martin.haardt}@tu-ilmenau.de

The authors gratefully acknowledge the partial support of the German Research Foundation (Deutsche Forschungsgemeinschaft, DFG) under contract no. WO 1442/1–1 and WO 1442/1–2.